

Asymmetrical ligand binding by abscisic acid 8'- hydroxylase

Kotomi Ueno,^a Hidetaka Yoneyama,^b Masaharu Mizutani,^c Nobuhiro Hirai,^d and Yasushi Todoroki^{b,*}

^a The United Graduate School of Agricultural Science, Gifu University, Gifu 501-1193, Japan

^b Department of Applied Biological Chemistry, Faculty of Agriculture, Shizuoka University, Shizuoka
422-8529, Japan

^c Institute for Chemical Research, Kyoto University, Uji, Kyoto 611-0011, Japan

^d International Innovation Center, Kyoto University, Kyoto 606-8501, Japan

* Corresponding author. Phone&Fax: +81-54-238-4871. E-mail: aytodor@agr.shizuoka.ac.jp

Abstract

Abscisic acid (ABA), a plant stress hormone, has a chiral center (C1') in its molecule, yielding the enantiomers (1'S)-(+)-ABA and (1'R)-(-)-ABA during chemical synthesis. ABA 8'-hydroxylase (CYP707A), which is the major and key P450 enzyme in ABA catabolism in plants, catalyzes naturally occurring (1'S)-(+)-enantiomer, whereas it does not recognize naturally not occurring (1'R)-(-)-enantiomer as either a substrate or an inhibitor. Here we report a structural ABA analogue (AHI1), whose both enantiomers bind to recombinant *Arabidopsis* CYP707A3, in spite of stereo-structural similarity to ABA. The difference of AHI1 from ABA is the absence of the side chain methyl group (C6) and lack of the α,β -unsaturated carbonyl (C2'=C3'-C4'=O) in the six-membered ring. To explore which moiety is responsible for asymmetrical binding by CYP707A3, we synthesized and tested ABA analogues that lacked the each moiety. Competitive inhibition was observed for the (1'R) enantiomers of these analogues in the potency order of (1'R,2'R)-(-)-2',3'-dihydro-4'-deoxo-ABA ($K_I = 0.45 \mu\text{M}$) > (1'R)-(-)-4'-oxo-ABA ($K_I = 27 \mu\text{M}$) > (1'R)-(-)-6-nor-ABA and (1'R,2'R)-(-)-2',3'-dihydro-ABA (no inhibition). In contrast to the (1'R)-enantiomers, the inhibition potency of the (1'S)-analogues declined with the saturation of the C2',C3'-double bond or with the elimination of the C4'-oxo moiety. These findings suggest that the C4'-oxo moiety coupled with the C2',C3'-double bond is the significant key functional group by which ABA 8'-hydroxylase distinguishes (1'S)-(+)-ABA from (1'R)-(-)-ABA.

1. Introduction

Abscisic acid (ABA) is a plant hormone involved in stress tolerance, stomatal closure, flowering, seed dormancy, and other physiological events.¹⁻³ In addition, it was reported recently that ABA should function as an endogenous proinflammatory cytokine in human.⁴ Endogenous levels of ABA in plants are properly and cooperatively controlled by the biosynthesis, transportation, and catabolic inactivation, in response to environmental changes.¹⁻³ A natural or artificial chemical which perturbs this highly controlled system is promising not only as chemical probes for the mechanism of ABA action,⁵ but also for practical purposes because of its potential use in agricultural, horticultural, or clinical. Although ABA is registered as a pesticide (plant growth regulator), its practical use has been limited mainly due to its weak effect in field trial.⁶ The weak effect is considered to be due to the rapid inactivation through biodegradation. Catabolic inactivation of ABA is mainly controlled by ABA 8'-hydroxylase, which is the cytochrome P450 catalyzing the C8'-hydroxylation of ABA into 8'-hydroxy-ABA and its more stable tautomer phaseic acid which has much lower hormonal activity than ABA.⁷ ABA 8'-hydroxylase was identified as CYP707A1-4 in the model plant, *Arabidopsis thaliana*, in 2004,^{8,9} and since then many CYP707A isozymes have been found in various plants.¹⁰⁻¹³ Gene knockdown and overexpression studies suggest that ABA 8'-hydroxylase is a key enzyme for controlling ABA concentration during water deficit stress or dormancy maintenance and breaking.^{14,15} To chemically control ABA 8'-hydroxylation in plants, we are developing stable ABA analogues¹⁶⁻¹⁸ and specific inhibitors¹⁹⁻²¹ against ABA 8'-hydroxylase. For effectively designing these chemicals, we need to know the substrate binding and enzyme reaction mechanisms in detail. Because the 3D structure of ABA 8'-hydroxylase has still not been investigated, we have attempted to explore the active site from the ligand side using many ABA analogues that we have developed.¹⁹⁻²¹ In the process of this research, we found AHI1, a compound which can be a key molecule to uncover the mechanism of asymmetrical ligand recognition by ABA 8'-hydroxylase.

ABA has a chiral center (C1') in its molecule, yielding the enantiomers (1'S)-(+)-ABA and (1'R)-(-)-ABA during chemical synthesis (Figure 1). All the naturally occurring ABA has the (1'S)-configuration, and its counterpart has never been detected in plants.¹⁻³ Nevertheless, many reports demonstrated that both enantiomers showed similar hormonal activities in many assay systems,²² suggesting that plants have a mechanism which permits the isomer that is not occurring naturally to mimic the endogenous hormone. However, the mechanism by which this occurs is not yet known. All the ABA-binding proteins ever identified, including three ABA receptors,²³⁻²⁵ cannot bind (1'R)-(-)-ABA. ABA 8'-hydroxylase also stereospecifically catalyzes naturally occurring (1'S)-(+)-ABA.⁹ (1'R)-(-)-ABA is not recognized by ABA 8'-hydroxylase as either a substrate or an inhibitor. If we understand what structural properties of ABA cause the asymmetrical recognition by ABA 8'-hydroxylase, we can speculate on a mechanism by which an ABA-binding protein does or does not discriminate between each enantiomer of ABA. This knowledge will be very useful to design an asymmetrical probe (agonist or antagonist) for an ABA-binding protein.

AHI1 is a lead compound for the development of an ABA 8'-hydroxylase inhibitor.²⁰ AHI1 was designed to be in *cis* between the side chain and the C2'-methyl (C7'); in this case, C7' of AHI1 mimics well the steric orientation of that of ABA (Figure 1). Therefore, an enantiomer of AHI1 has the (1'S,2'S) or (1'R,2'R) configuration; the former corresponds to (1'S)-(+)-ABA. As described in detail later, we found that both the enantiomers of AHI1 bind to the active site of ABA 8'-hydroxylase, contrary to the case of ABA, in spite that the 2D and 3D structures of AHI1 are very similar to those of ABA (Figure 1). The structural differences between AHI1 and ABA are the absence of the methyl group (C6) in the side chain and the α,β -unsaturated carbonyl group (C2'=C3'-C4'=O) in the six-membered ring. Therefore, either of these moieties should play an important role in chiral recognition of ABA by ABA 8'-hydroxylase. For clarifying which moiety is mainly responsible, we prepared optically pure 6-nor-ABA, 2',3'-dihydro-ABA, 4'-deoxo-ABA, 2',3'-dihydro-4'-deoxo-ABA, and *epi*-

AHI1 in addition to AHI1, and examined their binding potency to the ABA 8'-hydroxylase active site. Because cytochrome P450 enzymes perform numerous functions including metabolism of drugs in human, sterol synthesis in microorganisms, and as well as biosynthesis of natural products and hormone metabolisms in plants, they are targets for the development of drugs for human therapies or pesticides for agricultural purposes.²⁶ Many drugs and pesticides targeting P450 enzymes are asymmetrical, and generally each enantiomer has a different effect on the target enzyme reaction. Although the present study is an example for probing a mechanism of asymmetrical recognition of a specific ligand by a specific enzyme, it may give a general idea for asymmetric interaction of a small molecule with an endogenous macromolecule.

2. Results and Discussion

2.1. Preparation of optically pure AHI1 and determination of the absolute configurations.

Racemic AHI1, which was synthesized as reported previously,²⁰ was optically resolved into (+)- and (-)-enantiomers using HPLC with a chiral column. As described above, the absolute configurations of optically pure AHI1 are (1'*S*,2'*S*) or (1'*R*,2'*R*); the (1'*S*,2'*S*)-AHI1 corresponds to (*S*)-(+)-ABA, whereas the (1'*R*,2'*R*)-AHI1 corresponds to (*R*)-(-)-ABA (Figure 1). We determined the absolute configuration of AHI1 by converting it to the same compound **2** as that derived from ABA. The overall scheme is shown in Figure 2. Because the reactions in this scheme do not include any substitution reactions at C1' to induce chiral inversion or racemization, the C1' configurations should be maintained. Oxidative cleavage of (+)-AHI1 gave the aldehyde **1** which was converted to the ketone **2** with methylmagnesium bromide and subsequent pyridinium dichromate (PDC) oxidation. These reactions have no effect on the absolute configuration at C2'; therefore, the relative configuration of compound **2** derived from (+)-AHI1 is (1'*S**,2'*S**). On the other hand, sodium borohydride reduction of the methyl ester of (+)-ABA

(Me ABA) in tetrahydrofuran (THF) proceeded to give **3** as a diastereomeric mixture at C4' and the methyl esters of 1',4'-*trans*-diol-ABA (**4**) and 1',4'-*cis*-diol-ABA (**5**). Deoxygenation of **3** with tributyltin hydride via thiono esterification yielded the methyl ester of 2',3'-dihydro-4'-deoxo-ABA as a 2*E*/2*Z* mixture including little diastereomers. Oxidative cleavage of the ester with NaIO₄ and OsO₄ after alkaline hydrolysis yielded the single compound, which agreed with **2** derived from (+)-AHI1, by spectrometric and chiral HPLC analyses. Therefore, the absolute configuration of C1' in **2** is *S*. Finally we determined the absolute configuration of (+)-AHI1 as (1'*S*,2'*S*); that is, (+)-AHI1 corresponds to (1'*S*)-(+)-ABA, the naturally occurring ABA, whereas (-)-AHI1 corresponds to (*R*)-(-)-ABA, the naturally not occurring form.

The fact that compound **2** was obtained from (+)-Me ABA with little diastereomeric impurity, means that the reduction at C2' of (+)-Me ABA proceeded stereospecifically. The hydride addition must have occurred from the same side as the 1'-hydroxyl group, which is less bulkier than the side chain.

The favored conformation of AHI1 is similar to that of ABA; it is a chair form with the axial side chain and equatorial C7', as previously reported (Figure 1B).²⁰ Therefore, we can discuss the effect of the local structural difference between AHI1 and ABA on the affinity for the enzyme active site.

2.2. Both enantiomers of AHI1 act as competitive inhibitors

We estimated binding potency of optically pure AHI1 to the active site of ABA 8'-hydroxylase, by examining its competitive inhibition potency against the recombinant *Arabidopsis* CYP707A3 enzyme. (+)-AHI1 acted as a competitive inhibitor of CYP707A3 with a K_I value of 1.28 μ M (Table 1), which is slightly higher than the K_M value (0.71 μ M) of (+)-ABA. This suggests that the affinity of (+)-AHI1 for the enzyme active site is somewhat weaker than that of (+)-ABA. AHI1 does not have the methyl group (C6) in the side chain and the enone moiety (C2'=C3'-C4'=O) in the ring of ABA (Figure 1).

Because the elimination of C6 in (+)-ABA does not affect binding to the active site,¹⁹ the low affinity of (+)-AHI1 is likely a consequence of the absence of the enone moiety in the ring. (+)-AHI1 was converted into unidentified UV-absorbing compounds during the enzymatic reaction. Because this conversion was reduced by the addition of (+)-ABA, the UV-absorbing compounds are presumed to be the enzymatic reaction products. This suggests that (+)-AHI1 acts as a substrate of CYP707A3.

(-)-AHI1 also acted as a competitive inhibitor, in spite of its similarity to (-)-ABA. Its K_I value was 0.30 μM (Table 1), which was lower than that of (+)-AHI1 and the K_M value of (+)-ABA. This means that (-)-AHI1 binds to the active site more strongly than (+)-AHI1 and (+)-ABA. (-)-AHI1 yielded no enzyme reaction product, meaning that it was an inhibitor but not a substrate of CYP707A3. The absence of the ring enone may allow (1'*R*)-enantiomers to bind to the active site, in a manner not equal to that of (+)-ABA, as described later in detail.

2.3. Preparation of probes for exploring which functional group of (-)-ABA disturbs binding to the active site

We prepared four ABA analogues to identify the key functional group of (-)-ABA that is responsible for disturbing binding to the active site: 6-nor-ABA;¹⁹ 2',3'-dihydro-ABA;²⁷ 4'-deoxo-ABA;²⁸ and 2',3'-dihydro-4'-deoxo-ABA.²⁹ Optically pure 6-nor-ABA was synthesized as reported previously.¹⁹ 4'-Deoxo-ABA and 2',3'-dihydro-4'-deoxo-ABA have never been asymmetrically prepared, and the known synthesis of optically pure 2',3'-dihydro-ABA was complex and time consuming. We synthesized these three analogues using the new synthetic routes (Figure 2), in which the starting compound is ABA; therefore, the absolute configuration of the analogues at C1' depends on that of ABA.

Compounds **3**, **4** and **5** were prepared from Me ABA with NaBH₄ in THF described above. Oxidation of (1'*S*,2'*S*)-**3** with PDC and subsequent alkaline hydrolysis produced (1'*S*,2'*S*)-(+)-2',3'-dihydro-ABA. (1'*R*,2'*R*)-(-)-2',3'-dihydro-ABA was prepared from (-)-ABA by the same method as the (+)-enantiomer. (1'*S*,2'*S*)-(+)-2',3'-dihydro-4'-deoxo-ABA was synthesized described above. (1'*S*)-(+)-4'-deoxo-ABA was synthesized by elimination of the 4'-hydroxyl group of **5** with palladium-catalyzed borohydride reduction via the allylic carbonate before alkaline hydrolysis. The (-)-enantiomers of 2',3'-dihydro-4'-deoxo-ABA and 4'-deoxo-ABA were prepared by optical resolution of their racemates that were synthesized from (±)-ABA in the same manner as the (+)-enantiomer. The NMR and MS spectral data of these analogues are consistent with those reported previously.²⁷⁻²⁹ Compared to the absolute configuration of the starting compound ABA, all the (+)-probes have the 1'*S* configuration, whereas all the (-)-probes have the 1'*R* configuration.

The favored conformation of the ring-modified probes was estimated to be a chair (half-chair in the case of 4'-deoxo-ABA) with the axial side chain on the basis of the NMR (NOE difference spectra and NOESY experiments) and theoretical analysis (Figure 3 and Table 2). Therefore, we can discuss the effect of the local structural difference between these probes and ABA on the affinity for the enzyme active site.

2.4. The binding potency of (+)- and (-)-probes to the CYP707A3 active site

Both enantiomers of the probes were tested their ability to inhibit the 8'-hydroxylation reaction by recombinant CYP707A3, except for (+)-6-nor-ABA whose activity was reported previously.¹⁹ The results are summarized in Table 1. The mode of inhibition of all analogues with inhibition potency was competitive (Figure 4A,B). (-)-6-Nor-ABA did not inhibit the enzyme, unlike (+)-6-nor-ABA. This suggests that the methyl group of the side chain has nothing to do with chiral recognition by

CYP707A3. Therefore, the key moieties affecting the affinity for CYP707A3 should be the C4'-oxo, the C2',C3'-double bond, or both.

Each enone-modified (–)-probes exhibited a different affinity. The most active one was (1'R,2'R)-(–)-2',3'-dihydro-4'-deoxo-ABA with an K_i value of 0.45 μM (Table 1), indicating that this probe binds to the active site as effectively as (–)-AHI1. The structural difference of (–)-2',3'-dihydro-4'-deoxo-ABA from (–)-AHI1 is the existence of the side chain methyl (C6), suggesting that C6 in the (–)-enantiomer has little effect on binding to the active site, similarly to the (+)-enantiomer. (–)-2',3'-Dihydro-ABA exhibited no inhibitory activity, suggesting that the C4'-oxo moiety rather than the C2',C3'-double bond in (–)-ABA disturbs binding to the active site. (–)-4'-Deoxo-ABA functioned weakly as an inhibitor, although its activity was one-sixtieth that of (–)-2',3'-dihydro-4'-deoxo-ABA. This suggests that the presence of the C2',C3'-double bond also results in loss of affinity. Thus (–)-ABA cannot bind to the active site of CYP707A3 owing to the 4'-oxo moiety coupled with the C2',C3'-double bond.

All the enone-modified (+)-probes acted as weak inhibitors of CYP707A3. The absence of the ring enone in (+)-ABA results in a decrease affinity, although not necessarily significant.

2.5. A putative mechanism of asymmetrical ligand binding by CYP707A3

Biological chiral recognition toward a substrate with one stereocenter involves at least three locations interacting with one and more receptor sites.³⁰ ABA has three oxygenated functional groups: C1-carboxyl, C1'-hydroxyl, and C4'-oxo moiety. The C1-carboxyl in (+)-ABA is an absolutely essential moiety, including the (2Z,4E) geometry of the side chain, for binding to the CYP707A3 active site.¹⁹ As described above, the C4'-oxo in (+)-ABA is also related to binding to the active site. On the other hand, the C1'-hydroxyl has nothing to do with binding to the active site.¹⁹ Thus two of the three locations in (+)-ABA are the C1-carboxyl and C4'-oxo moieties, and the third location is not an oxygenated functional group. As shown in Figure 1B, the major difference between (+)- and (–)-ABA

is the location of the axial C6'-methyl (C8') in the ring. Because C8' is the site hydroxylated by CYP707A3, it is reasonable to assume that C8' functions as a third location for the chiral recognition by CYP707A3. If the C1- and C4'-moieties of (-)-ABA interact with the active site similarly to (+)-ABA, the C8' of (-)-ABA cannot occupy the same location as that of (+)-ABA. However, the binding interaction is not required to occur in all three locations if the asymmetrical discrimination is not necessary. Simply, this may be the reason why (-)-AHI1 and (-)-2',3'-dihydro-4'-deoxo-ABA, which lacks the C4'-oxo function, can bind to the active site. These two probes may be mainly anchored to the active site through the C1-carboxyl, and reinforce the affinity by relatively non-specific, hydrophobic interactions by the lipophilic ring, although this binding manner should be different from that of (+)-ABA. In that case, (-)-ABA cannot bind to the active site in the similar manner to these probes, probably because the C4'-oxo moiety decreases the lipophilicity of the ring, or it has an unfavorable electrostatic interaction with the active site. This hypothesis led us to speculate that an ABA analogue with the same side chain as that of ABA, if its six-membered ring has no oxygenated functional group except for the C1'-hydroxyl group, can bind to the CYP707A3 active site, independent of its C1'-configuration. Therefore, we synthesized and tested the epimer of AHI1 (*epi*-AHI1). *epi*-AHI1 should adopt a chair conformation with the equatorial side chain because of the 1,3-diaxial repulsion between C7' and C8' (Figure 5A and Table 2). Our previous study¹⁹ suggests that ABA analogues with the C4'-oxo moiety are required to have the axial side chain in the favored conformation for a good affinity to the active site. Therefore, *epi*-AHI1 can be a good probe for testing our hypothesis about the binding mechanism of ABA analogues with no C4'-oxo moiety.

2.6. Synthesis of *epi*-AHI1

Racemic *epi*-AHI1 was prepared using the same synthetic route of AHI1 that was reported previously (Figure 5B).²⁰ Briefly, the racemic compound **6** generated by acetylide anion attack to trimethylcyclohexanone was reduced with sodium bis(methoxyethoxy)aluminum dihydride (SMEAH),

de-protected with AcOH and H₂O, and oxidized with PDC to give the racemic aldehyde **7**. The Horner-Emmons reaction of **7** and subsequent alkaline hydrolysis gave *epi*-AHI1 with a total yield of 1.5%. The relative configurations of *epi*-AHI1 were determined on the basis of those of the compound **6**. The introduction of the side chain to trimethylcyclohexanone yielded the compound **6** as the minor diastereomer. Because in this reaction the major diastereomer was the synthetic precursor of AHI1, the end product derived from the compound **6** must be the epimer of AHI1. Racemic *epi*-AHI1 was optically resolved to obtain (+)- and (-)-enantiomers using chiral HPLC, although the absolute configurations of optically pure *epi*-AHI1 have never been determined.

2.7. Both enantiomers of *epi*-AHI1 act as a substrate of CYP707A3

In the inhibition assay using recombinant CYP707A3, both enantiomers of *epi*-AHI1 competitively inhibited the enzyme reaction. The K_I values for (+)- and (-)-*epi*-AHI1 were 2.50 μ M and 1.63 μ M, respectively (Table 1, Figure 4C). This suggests that the affinity of both *epi*-AHI1 enantiomers for the enzyme active site is almost equivalent to that of AHI1 and 2',3'-dihydro-4'-deoxo-ABA. Each enantiomer of *epi*-AHI1 was converted into distinct UV-absorbing product during the enzyme reaction. The product from (+)-*epi*-AHI1 showed a quasimolecular ion $[M + Na]^+$ at m/z 275 in the ESI-TOF-MS (positive mode) analysis; it has 14 additional mass unit compared to (+)-*epi*-AHI1. This suggests that a methylene group of *epi*-AHI1 was oxidized to a carbonyl group. Cytochrome P450s catalyze not only hydroxylation but also carbonylation and carboxylation.²⁶ In fact, P450-catalyzed oxidation of ABA includes the further oxidation of the first product 8'-hydroxy-ABA to 8'-oxo-ABA in maize cells.³¹ Therefore, it is reasonable to assume that CYP707A3 catalyzes the two-step oxidation of *epi*-AHI1. On the other hand, the enzyme product of (-)-*epi*-AHI1 showed a quasimolecular ion at m/z 269 (positive mode), which cannot lead us to the estimated molecular structure.

In spite of its different conformation from that of AHI1 and other C4'-deoxo-probes prepared in this study, both enantiomers of *epi*-AHI1 occupied the active site of CYP707A3 to be converted to the enzyme reaction products. These results confirm our speculation that an ABA analogue with the same side chain as that of ABA, if its six-membered ring has no oxygenated functional group except for the C1'-hydroxyl group, can bind to the CYP707A3 active site, independent of its C1'-configuration. In the previous study, we developed AHI4 as a strong non-azole inhibitor of ABA 8'-hydroxylase.²¹ The epimer of AHI4 at C2', *epi*-AHI4, adopts the similar ring conformation to *epi*-AHI1. Nevertheless, *epi*-AHI4 did not exhibit the enzyme inhibition activity.²¹ *epi*-AHI4 has a hydroxyl group instead of the C8' of *epi*-AHI1; therefore, the ring of AHI4 should be more hydrophilic than that of AHI1. This may be the reason why *epi*-AHI4 did not act as an inhibitor of the enzyme.

3. Conclusions

Plant P450 CYP707A3, ABA 8'-hydroxylase, binds enantioselectively (+)-ABA but not (-)-ABA, whereas the enzyme binds both enantiomers of AHI1. We focused on the structural differences between the two compounds, and designed and synthesized four asymmetrical molecular probes for exploring a key functional group of (-)-ABA responsible for disturbing binding to the active site: 6-nor-ABA; 2',3'-dihydro-ABA; 4'-deoxo-ABA; and 2',3'-dihydro-4'-deoxo-ABA. The structure-activity studies using these probes suggested that the C4'-carbonyl moiety coupled with the C2',C3'-double bond is a significant key function for asymmetrical binding of ABA by ABA 8'-hydroxylase.

4. Experimental

4.1. Chemicals

(+)-ABA was a gift from Toray Industries Inc., Tokyo, Japan. Phaseic acid was prepared as reported previously.³² Synthesis of (±)-AHI1 was reported previously.²⁰ Compounds 1-7, enone-modified ABA analogues and (±)-*epi*-AHI1 were prepared by the synthetic route shown as Figures 2 and 5, and by described below. Optical resolutions of racemic AHI1 and *epi*-AHI1 were performed using chiral HPLC. Racemic enone-modified ABA analogues were synthesized from (±)-ABA, and (+)-ABA was also converted to enone-modified ABA analogues by the same manners to determine the absolute configuration of these analogues. (1'*R*,2'*R*)-2',3'-dihydro-ABA was prepared from (-)-ABA by the same method as the counterpart, and (1'*R*)-enantiomers of 4'-deoxo-ABA and 2',3'-dihydro-4'-deoxo-ABA were obtained by optical resolution of the racemates. ¹H NMR spectra were recorded with tetramethylsilane as the internal standard using a JEOL JNM-EX 270 NMR spectrometer (270 MHz). For clarity, the atoms of all the compounds with the carbon skeleton of ABA were numbered as in ABA for peak assignments. High resolution mass spectra (HRMS) were obtained with a JEOL JMS-DX 303 HF mass spectrometer and with a JEOL JMS-T100LC "AccuTOF". Optical rotation was recorded with a Jasco DIP-1000 digital polarimeter. Column chromatography was performed on silica gel (Wakogel C-200). Purity in two solvent systems (H₂O-MeOH and H₂O-MeCN) was determined using a Shimadzu LC-10ADVP instrument, and all final compounds were >97% pure (see Supporting Information for details).

4.2. (+)- and (-)-AHI1

(±)-AHI1²⁰ (45 mg, 0.19 mmol) were subjected to chiral HPLC under the following conditions: column, Chiralpak AD-H (250 × 4.6 mm, Daicel); solvent, 8% 2-propanol in *n*-hexane containing 0.1% trifluoroacetic acid (TFA); flow rate, 1.0 ml min⁻¹; detection, 254 nm. The materials at *t*_R 8.2 and 11.6 min were collected to give (+)-AHI1 (22 mg, 92 μmol) and its (-)-enantiomer (22 mg, 92 μmol) with

an optical purity of 99.9 and 95.9%, respectively. (+)-AHI1: $[\alpha]_D^{29} +71.4$ (MeOH, c 1.083); (–)-AHI1; $[\alpha]_D^{29} -69.2$ (MeOH, c 1.117).

4.3. Synthesis of 2',3-dihydro-4'-deoxo-ABA

4.3.1. (*E*)-3-((1*S*,2*S*)-1'-hydroxy-2',6',6'-trimethylcyclohexyl)acrylaldehyde (1**).** NaIO₄ (20 mg, 93 μmol) was added to a solution of (+)-AHI1 (2.2 mg, 9.2 μmol) in 1,4-dioxane (0.1 mL) and H₂O (0.1 mL). A solution of OsO₄ in H₂O (7.1 μM solution, 5 μL, 36 μmol) was added, the mixture was stirred for 14 h at room temperature. NaIO₄ (25 mg, 0.12 mmol) and a solution of OsO₄ in H₂O (0.11 mL, 0.78 mmol) was then added to a mixture, and stirred for 12 h at room temperature. After being quenched with 2-propanol (0.5 mL), the resulting mixture was extracted with EtOAc (1.5 mL × 10). The organic layer was washed with brine and H₂O, dried over Na₂SO₄, and concentrated. The residual oil was purified by column chromatography (Sep-Pak Plus Silica cartridge) with 5% EtOAc in hexane to obtain **1** (1.0 mg, 5.1 μmol, 55%) as white amorphous solid. ¹H NMR (270 MHz, CDCl₃): δ 0.79 (3H, d, $J = 6.9$ Hz, H₃-7'), 0.82 (3H, s, H₃-9'), 1.09 (3H, s, H₃-8'), 1.20-1.32 and 1.45-1.72 (6H, m, H₂-3', H₂-4' and H₂-5'), 1.96 (1H, ddq, $J = 13.2, 6.9$ and 3.6 Hz, H-2'), 6.43 (1H, dd, $J = 15.5$ and 7.9 Hz, H-2) 7.12 (1H, d, $J = 15.5$ Hz, H-3) and 9.63 (1H, d, $J = 7.9$ Hz, H-1); HRMS (EI) calcd for C₁₂H₂₀O₂ [M]⁺ 196.1463, found 196.1461.

4.3.2. (*E*)-4-((1*S*,2*S*)-1'-hydroxy-2',6',6'-trimethylcyclohexyl)but-3-en-2-one (2**) from **1**.** A solution of methylmagnesium bromide (35% in Et₂O, *ca* 3 M, 80 μL, 0.24 mmol) was added to a solution of the aldehyde **1** (1.0 mg, 5.1 μmol) in dry THF (0.1 mL) at –10 °C under Ar. The mixture was stirred for 20 min, and H₂O (10 mL) was then added to the mixture. The solution was extracted with EtOAc (2 mL × 5), the organic layer was washed with brine and H₂O, dried over Na₂SO₄ and concentrated. The residual oil was chromatographed on silica gel with 40% EtOAc in hexane to give

the alcohol (0.8 mg, 3.8 μmol) as colorless oil. PDC (3 mg, 8 μmol) and Celite were added to a solution of the alcohol (0.8 mg, 3.8 μmol) in dry CH_2Cl_2 (0.2 mL), and the mixture was stirred for 16 h at room temperature. The mixture was filtered with Celite and the filtrate was concentrated. The residual oil was purified by column chromatography on silica gel with 15% EtOAc in hexane and with a Sep-Pak Plus C18 cartridge using 70% MeOH in H_2O to obtain **2** (0.4 mg, 2.1 μmol , 40%) as colorless oil. ^1H NMR (270 MHz, CDCl_3): δ 0.77 (3H, d, $J = 6.6$ Hz, $\text{H}_3\text{-7}'$), 0.80 (3H, s, $\text{H}_3\text{-9}'$), 1.07 (3H, s, $\text{H}_3\text{-8}'$), 1.16-1.67 (6H, m, $\text{H}_2\text{-3}'$, $\text{H}_2\text{-4}'$ and $\text{H}_2\text{-5}'$), 1.93 (1H, ddq, $J = 13.5$, 6.6 and 3.2 Hz, $\text{H-2}'$), 2.28 (3H, s, $\text{H}_3\text{-1}$), 6.40 and 7.10 (each 1H, d, $J = 15.8$ Hz, H-3 and H-4); HRMS (EI) calcd for $\text{C}_{13}\text{H}_{22}\text{O}_2$ $[\text{M}]^+$ 210.1620, found 210.1618.

4.3.3. (1'S*,2'S*)-(\pm)-2. Compound (\pm)-**1**²⁰ (4.3 mg, 22 μmol) gave (\pm)-**2** (3.3 mg, 16 μmol , 73%) in the similar manner to **1**.

4.3.4. Methyl (1'S*,2'S*)-(\pm)-2',3-dihydro-4'-hydroxy-abscisate (3) and methyl (1'S*)-(\pm)-1',4'-cis/trans-diol-abscisate (4 and 5). Racemic ABA (0.36 g, 1.4 mmol) was dissolved in MeOH (10 mL) and a solution of (trimethylsilyl)diazomethane (2.0 M in hexanes, 5 mL, 10 mmol) was added to the solution with cooling. After removal MeOH and hexane in vacuo, the residue was redissolved in dry THF (15 mL), and NaBH_4 (0.22 g, 5.9 mmol) was added to the solution. The mixture was stirred for 30 h at room temperature in the dark, and brine was added to the resulting mixture with cooling to quench the reaction. After separating the THF layer, the aqueous layer was extracted with EtOAc (20 mL \times 5). The THF and EtOAc layers were combined, washed with saturated NH_4Cl and H_2O , dried over Na_2SO_4 , and concentrated. The residual oil was purified by column chromatography on silica gel with 20-40% EtOAc in hexane to give methyl (\pm)-1',4'-trans-diol-abscisate (**4**, 0.13 g, 0.48 mmol, 35%) as colorless oil, (1'S*,2'S*)-(\pm)-**3** (0.18 g, 0.65 mmol, 47%) as white amorphous solid, and methyl (\pm)-1',4'-cis-diol-abscisate (**5**, 0.054 g, 0.19 mmol, 14%) as colorless oil. ^1H NMR and MS spectra of **4** and **5** were considered with a previous report.³³ Data of **3** (1:1 diastereomeric mixture at C4'). ^1H

NMR (270 MHz, CDCl₃): δ 0.81 (3H, d, J = 6.6 Hz, H₃-7'), 0.82 (3H, s, H₃-9'), 1.10 and 1.27 (3H, s, H₃-8'), 1.22-1.31, 1.45-1.56, 1.69-1.77 and 1.87-1.92 (4H, m, H₂-3' and H₂-5'), 2.01 and 2.03 (3H, d, J = 1.0 Hz, H₃-6), 2.05 and 2.37 (1H, m, H-2'), 4.03 and 4.13 (1H, m, H-4'), 5.70 (1H, broad s, H-2), 6.28 and 6.42 (1H, d, J = 16.2 Hz, H-5), 7.76 and 7.80 (1H, d, J = 16.2 Hz, H-4); HRMS (EI) calcd for C₁₆H₂₆O₄ [M]⁺ 282.1831, found 282.1829.

4.3.5. (1'S,2'S)-(+)-3. (+)-ABA (11 mg, 41 μ mol) was converted to (1'S,2'S)-(+)-**3** (5.0 mg, 18 μ mol, 44%) by the same method described above.

4.3.6. (1'S*,2'S*)-(\pm)-2',3-dihydro-4'-deoxo-ABA. (1'S*,2'S*)-(\pm)-**3** (0.16 g, 0.57 mmol) was dissolved in dry CH₂Cl₂ (3 mL), and dry pyridine (0.7 mL) and 4-dimethylaminopyridine (4-DMAP, 76 mg, 0.62 mmol) were added to the solution. Phenyl chlorothioformate (1 mL, 7.3 mmol) was added to the solution at 0 °C, and the resulting mixture was stirred for 105 min at room temperature in the dark. After quenching the reaction with brine, the CH₂Cl₂ layer was separated, and the aqueous layer was extracted with EtOAc (10 mL \times 5). The CH₂Cl₂ and EtOAc layers were combined, washed with saturated NaHCO₃, 0.1 M HCl, brine and H₂O, dried over Na₂SO₄, and concentrated. The residual oil was purified by column chromatography on silica gel with 5% EtOAc in hexane to give the thiono ester (0.21 g) as yellow oil. The thiono ester (0.11 g) was dissolved in dry toluene (3 mL) and warmed to 70 °C. A solution of 2,2'-azobisisobutyronitrile (7.3 mg, 45 μ mol) and tri-*n*-butyltin hydride (0.2 mL, 0.76 mmol) in toluene (1.5 mL) was added dropwise to the solution over 3 min, and the resulting mixture was stirred for 2 h at 70 °C under Ar. The toluene solution was applied onto silica gel column and products were eluted with 8% EtOAc in hexane. The eluate was concentrated, the residue (34 mg) was redissolved in MeOH (1.5 mL), and 1 M NaOH (1.5 mL, 1.5 mmol) was added to the solution. After stirring for 16.5 h, the solution was filled up to 50 mL with brine. The resulting solution was extracted with hexane (5 mL \times 3), and the aqueous layer was extracted with EtOAc (8 mL \times 5) after acidifying to pH 1 with 1 M HCl. The EtOAc layer was washed with H₂O, dried over

Na₂SO₄ and concentrated. The residual oil was purified using silica gel column chromatography with 15% EtOAc in hexane containing 0.1% AcOH and Sep-Pak Plus C18 cartridges with 65-80% MeOH in H₂O containing 0.05% AcOH to obtain (1'S*,2'S*)-(±)-2',3'-dihydro-4'-deoxo-ABA (9.6 mg, 38 μmol, 15%) as colorless oil. The ¹H NMR data was consistent with that reported previously.²⁹ UV λ_{max} (MeOH) nm (ε): 262.2 (17,400).

4.3.7. (1'S,2'S)-(+)-2',3'-dihydro-4'-deoxo-ABA. (1'S,2'S)-(+)-3 (3.8 mg, 14 μmol) was converted to (2E/2Z)-(1'S,2'S)-(+)-2',3'-dihydro-4'-deoxo-ABA (2.8 mg, 11 μmol, 79%) by the same method. The 2E/2Z isomer (350 μg, 1.3 μmol) was purified by column to obtain (1'S,2'S)-(+)-2',3'-dihydro-4'-deoxo-ABA (267 μg, 1.1 μmol, 85%) as a colorless oil. HRMS (EI) calcd for C₁₅H₂₄O₃ [M]⁺ 252.1725, found 252.1726.

4.3.8. (1'R,2'R)-(-)-2',3'-dihydro-4'-deoxo-ABA. (1'S*,2'S*)-(±)-2',3'-dihydro-4'-deoxo-ABA (2.7 mg, 11 μmol) was subjected to chiral HPLC using the following conditions: column, Chiralpak AD-H (250 × 4.6 mm, Daicel); solvent, 11% 2-propanol in *n*-hexane containing 0.1% TFA; flow rate, 0.6 ml min⁻¹; detection, 254 nm. The materials at *t*_R 9.4 and 12.1 min were collected to give (1'S,2'S)-(+)-2',3'-dihydro-4'-deoxo-ABA (0.68 mg, 2.7 μmol) and its (1'R,2'R)-(-)-enantiomer (0.65 mg, 2.6 μmol) with an optical purity of 99.9 and 99.6%, respectively. (1'S,2'S)-(+)-2',3'-dihydro-4'-deoxo-ABA: [α]_D²⁸ +79.7 (MeOH, *c* 0.104); (1'R,2'R)-(-)-2',3'-dihydro-4'-deoxo-ABA; [α]_D²⁸ -82.0 (MeOH, *c* 0.0651). HRMS (EI) calcd for C₁₅H₂₄O₃ [M]⁺ 252.1725, found 252.1726.

4.4. (E)-4-((1'S,2'S)-1'-hydroxy-2',6',6'-trimethylcyclohexyl)but-3-en-2-one (2) from (2E/2Z)-(1'S,2'S)-(+)-2',3'-dihydro-4'-deoxo-ABA

(2*E*/2*Z*)-(1'*S*,2'*S*)-(+)-2',3'-dihydro-4'-deoxo-ABA (2.0 mg, 7.9 μmol) was converted to **2** (0.3 mg, 1.4 μmol , 18%) by oxidative cleavage with NaIO_4 and OsO_4 (described above). Compound **2** was analyzed by HPLC with the following conditions. ODS HPLC: column, Hydrosphere C18 (150 \times 6.0 mm, YMC); solvent, 75% MeOH in H_2O ; flow rate, 1.0 mL min^{-1} ; detection, 254 nm. The peak of compound **2** prepared from (+)-AHI1 agreed with that from (1'*S*)-(+)-ABA upon coinjection analysis (t_{R} 6.8 min). Chiral HPLC conditions: column, Chiralpak AD-H (250 \times 4.6 mm, Daicel); solvent, 8% 2-propanol in *n*-hexane containing 0.1% TFA; flow rate, 1.0 mL min^{-1} ; detection, 254 nm. The peaks at t_{R} 6.7 and 7.5 min were detected when the (\pm)-**2** was injected, whereas the peak from injected **2** was detected at t_{R} 6.5 min.

4.5. Synthesis of 2',3-dihydro-ABA

4.5.1. (1'*S,2'*S**)-(\pm)-2',3-dihydro-ABA.** A mixture of PDC (51 mg, 0.14 mmol) and Celite was wet with CH_2Cl_2 and added a solution of (1'*S**,2'*S**)-(\pm)-**3** (31 mg, 0.11 mmol) in dry CH_2Cl_2 (0.5 mL). The mixture was stirred for 15.5 h at room temperature, filtered with Celite, and eluted with CH_2Cl_2 and EtOAc. The eluate was concentrated and filtered through a short column of silica gel to remove celite before the residual crude oil was dissolved in MeOH (1 mL). A solution of NaOH in H_2O (1 M, 1.5 mL, 1.5 mmol) was added to the solution and the mixture was stirred for 5 h at room temperature in the dark. The resulting mixture was filled up to 40 mL with brine and extracted with hexane (5 mL \times 3). The aqueous layer was acidified with 1 M HCl to pH 1 and extracted with EtOAc (7 mL \times 7). The EtOAc layer was washed with H_2O , dried over Na_2SO_4 and concentrated. The residual oil was purified by silica gel column chromatography with 50-70% EtOAc in hexane containing 0.1% AcOH to give (1'*S**,2'*S**)-(\pm)-2',3'-dihydro-ABA (18 mg) as white amorphous solid, which was recrystallized from acetone-toluene to give colorless crystal (16 mg, 60 μmol , 55%). The ^1H NMR data was consistent with those reported previously²⁷. UV λ_{max} (MeOH) nm (ϵ): 259.8 (21,600).

4.5.2. (1'S,2'S)-(+)-2',3'-dihydro-ABA. Compound (+)-**3** (4.1 mg, 15 μ mol) was converted to (1'S,2'S)-(+)-2',3'-dihydro-ABA (2.2 mg, 8.2 μ mol, 57%) by the same manner. $[\alpha]_D^{26} +66.7$ (MeOH, *c* 0.145) (lit. (27) $[\alpha]_D +63.5$); HRMS (EI) calcd for C₁₅H₂₂O₄ [M]⁺ 266.1518, found 266.1519.

4.5.3. (1'R,2'R)-(-)-2',3'-dihydro-ABA. (-)-ABA (3.1 mg, 12 μ mol) was converted to (1'R,2'R)-(-)-2',3'-dihydro-ABA (0.84 mg, 3.2 μ mol, 26%) via (-)-**3** in the similar manner to (+)-enantiomer. $[\alpha]_D^{26} -59.8$ (MeOH, *c* 0.0461) (lit. (27) $[\alpha]_D -65.2$); HRMS (EI) calcd for C₁₅H₂₂O₄ [M]⁺ 266.1518, found 266.1521.

4.6. Synthesis of 4'-Deoxo-ABA

4.6.1. (\pm)-4'-Deoxo-ABA. Anhydrous pyridine (0.5 mL) and 4-DMAP (23 mg, 0.19 mmol) was added to a solution of **5** (54 mg, 0.19 mmol) in dry CH₂Cl₂ (1 mL), which was cooled to 0 °C. Chloroformic acid methyl ester (0.4 mL, 5.2 mmol) was added to the solution, and the mixture was stirred for 30 min at room temperature. After quenching with H₂O at 0 °C and adding brine, the resulting mixture was extracted with EtOAc (6 mL \times 6). The organic layer was sufficiently washed with 0.1 M HCl, saturated NaHCO₃ and H₂O, dried over Na₂SO₄ and concentrated. The residual oil containing the methyl carbonate (58 mg) was dissolved in EtOAc, added hexane, and filtered through a short column of silica gel to remove pyridine. The eluate was concentrated, and the methyl carbonate (46 mg) was dissolved in 1,4-dioxane (1 mL). [Pd₂(dba)₃] \cdot CHCl₃ 2.7 mg (2.6 μ mol), *n*-Bu₃P (10% v/v in dioxane, 7 μ l, 2.8 μ mol) and a solution of NaBH₄ (15 mg, 0.39 mmol) in H₂O (0.15 mL) were added to the solution, and the mixture was stirred for 40 min at room temperature in the dark. Brine was added to the reaction mixture, and the solution was extracted with EtOAc (4 mL \times 8). The organic layer was washed with saturated NH₄Cl and H₂O, dried over Na₂SO₄ and concentrated. The residual oil was purified by column chromatography on silica gel with 10% EtOAc in hexane to give the ester

(26 mg), which dissolved in MeOH (1 mL). An aqueous solution of NaOH (1 M, 1 mL, 1 mmol) was added to the solution and stirred for 13.5 h at room temperature in the dark. The resulting mixture was filled up to 50 mL with brine, the solution was extracted with hexane. The aqueous layer was acidified to pH 1 with 1 M HCl before extracting with EtOAc (5 mL \times 4). The EtOAc layer was washed with H₂O, dried over Na₂SO₄ and concentrated. The residual oil was purified by column chromatography on silica gel with 20% EtOAc in hexane to obtain 4'-deoxo-ABA (18 mg, 70 μ mol, 46%) as colorless oil. The ¹H NMR and mass spectral data were consistent with those reported previously²⁸. UV λ_{\max} (MeOH) nm (ϵ): 262.2 (19,500).

4.6.2. (S)-(+)- and (R)-(-)-4'-Deoxo-ABA. (\pm)-4'-Deoxo-ABA (2.1 mg, 8.4 μ mol) was optically resolved by chiral HPLC using the following conditions: column, Chiralpak AD-H (250 x 4.6 mm, Daicel); solvent, 12% 2-propanol in *n*-hexane containing 0.1% TFA; flow rate, 0.6 ml min⁻¹; detection, 254 nm. The materials at t_R 9.4 and 10.6 min were collected to give (+)-4'-deoxo-ABA (0.84 mg, 3.4 μ mol) and its (-)-enantiomer (0.94 mg, 3.7 μ mol) with an optical purity of 99.8 and 99.9%, respectively. (+)-4'-deoxo-ABA: $[\alpha]_D^{29}$ +210.6 (MeOH, *c* 0.0843); HRMS (EI) calcd for C₁₅H₂₂O₃ [M]⁺ 250.1569, found 250.1570. (-)-4'-Deoxo-ABA; $[\alpha]_D^{29}$ -215.5 (MeOH, *c* 0.0937); HRMS (EI) calcd for C₁₅H₂₂O₃ [M]⁺ 250.1569, found 250.1564. By use of the same chiral HPLC conditions, the peak of (1'*S*)-4'-deoxo-ABA prepared from (+)-ABA was consistent with that of (+)-4'-deoxo-ABA, elucidating the (1'*S*) configuration of (+)-4'-deoxo-ABA.

4.7. Synthesis of *epi*-AHI1

4.7.1. (1'*S**,2'*R**)-(\pm)-3'-(1'-hydroxy-2',6',6'-trimethylcyclohexan-1'-yl)-propynol TBS ether (6).

A solution of *n*-butyllithium in *n*-hexane (1.6 mol l⁻¹, 9.0 mL, 14 mmol) was added dropwise to a solution of 2-propynyl-*tert*-butyldimethylsilyl (TBS) ether (3.6 g, 21 mmol) in dry THF (50 mL) at

-78 °C under Ar. The mixture was stirred for 40 min, and a solution of 2,2,6-trimethylcyclohexanone (1.0 g, 7.1 mmol) in dry THF (10 mL) was then added dropwise to the mixture at -78 °C. The reaction mixture was allowed to warm to -28 °C over 60 min before being quenched with water and extracted with EtOAc (30 mL × 4). The organic layer was washed with brine and H₂O, dried over Na₂SO₄ and concentrated. The residual oil was purified by column chromatography on silica gel with 2% EtOAc in hexane to obtain (1'S*,2'R*)-6 (0.13 g, 0.41 mmol, 5.7%) and its (1'S*,2'S*)-diastereomer (1.4 g, 4.6 mmol, 65%) as colorless oils. ¹H NMR (270 MHz, CDCl₃): δ 0.12 (6H, s, Si-Me₂), 0.91 (9H, s, *tert*-Bu-Si), 1.05 (3H, d, *J* = 6.9 Hz, H₃-7'), 1.07 and 1.08 (each 3H, s, H₃-8' and H₃-9'), 1.15-1.60 (6H, m, H₂-3', H₂-4' and H₂-5'), 1.89 (1H, m, H-2'), 4.16 (2H, s, H₂-1); HRMS (EI) calcd for C₁₈H₃₄O₂Si [M]⁺ 310.2328, found 310.2326.

4.7.2. (1'S*,2'R*)-(±)-3'-(1'-hydroxy-2',6',6'-trimethylcyclohexan-1'-yl)-propenal (7). A solution of sodium bis(2-methoxyethoxy)aluminum dihydride (SMEAH) in toluene (*ca* 70%, 0.85 mL, 3.1 mmol) was added dropwise to a solution of 6 (0.27 g, 0.88 mmol) in dry THF (25 mL) at 0 °C under Ar. The mixture was stirred for 2 h at room temperature before it was poured into H₂O. The solution was extracted with EtOAc (20 mL × 8) after saturated NaHCO₃ was added to the solution. The organic layer was washed with saturated NH₄Cl and H₂O, dried over Na₂SO₄ and concentrated. After the residual oil (0.24 g) was dissolved in THF (1 mL), 75% AcOH in H₂O (4 mL) was added to the solution, and the mixture was then stirred for 19 h at room temperature. The resulting mixture was filled up with brine to 40 mL before being extracted with EtOAc (7 mL × 8). The organic layer was washed substantially with saturated NaHCO₃ and H₂O, dried over Na₂SO₄ and concentrated. The residual oil was purified by column chromatography on silica gel with 30% EtOAc in hexane to give the alcohol (0.11 g, 0.54 mmol, 62%) as white amorphous solid. After PDC (0.25 g, 0.66 mmol) and Celite (0.5 g) were dissolved in dry CH₂Cl₂ (2 mL), a solution of the alcohol (0.11 g, 0.54 mmol) in dry CH₂Cl₂ (2 mL) was added and stirred for 4 h at room temperature. The mixture was filtered with Celite and the residue was eluted with CH₂Cl₂ (20 mL) and EtOAc (40 mL). The combined organic

solution was concentrated and the residual oil was purified by column chromatography on silica gel with 10-15% EtOAc in hexane to give **7** (76 mg, 0.39 mmol, 73%) as colorless oil. ¹H NMR (270 MHz, CDCl₃): δ 0.77 (3H, d, *J* = 6.6 Hz, H₃-7'), 0.86 (3H, s, H₃-8'), 1.07 (3H, s, H₃-9'), 1.20-1.38 and 1.49-1.72 (6H, m, H₂-3', H₂-4' and H₂-5'), 2.01 (1H, ddd, *J* = 12.6, 6.6 and 4.0 Hz, H-2'), 6.39 (1H, dd, *J* = 15.5 and 7.9 Hz, H-2), 7.82 (1H, d, *J* = 15.5 Hz, H-3), 9.61 (1H, d, *J* = 7.9 Hz, H-1); HRMS (EI) calcd for C₁₂H₂₀O₂ [M]⁺ 196.1463, found 196.1466.

4.7.3. (1'S*,2'R*)-(±)-*epi*-AHI1. A solution of ethyl di-*o*-tolylphosphonoacetate (0.39 g, 1.1 mmol) in dry THF (1 mL) was added to a solution of NaH (61 mg, 1.5 mmol) in dry THF (1 mL) at 0 °C under Ar. After being stirred for 25 min at 0 °C, the mixture was cooled to -78 °C and a solution of **7** (70 mg, 0.36 mmol) in dry THF (1 mL) was added. The reaction mixture was allowed to warm to -14 °C over 2 h before it was poured into saturated NH₄Cl and extracted with EtOAc (8 mL × 5). The organic layer was washed with H₂O, dried over Na₂SO₄ and concentrated. The residual oil was chromatographed using silica gel with 4-6% EtOAc in hexane to obtain a colorless oil (0.12 g) as crude products. The oil (0.12 g) was dissolved in MeOH (1.5 mL) and 1 M NaOH (1.5 mL, 1.5 mmol) was added to a solution. The mixture was stirred for 4.5 h at room temperature in the dark before it was filled up with H₂O to 30 mL and extracted with CH₂Cl₂ (4 mL × 3). The solution was extracted with EtOAc (7 mL × 5) after being acidified with 1 M HCl to pH 1. The EtOAc layer was washed with H₂O, dried over Na₂SO₄ and concentrated. The residual oil was prepurified by silica gel column chromatography with 20% EtOAc in hexane containing 0.1% AcOH and Sep-Pak Plus C18 cartridges with 80% MeOH in H₂O containing 0.05% AcOH to give a mixture of 2*E*/2*Z* isomers of *epi*-AHI1 (69 mg, 0.29 mmol) as colorless oil. The isomers were separated using HPLC as following conditions: column, YMC-Pack AQ311 (ODS, 100 × 6.0 mm I.D., YMC); solvent, 65% MeOH in H₂O containing 0.1% AcOH; flow rate, 1.0 mL min⁻¹; detection, 254 nm. The material at *t*_R 15.8 and 22.4 min were collected to give 2*E*-(±)-*epi*-AHI1 (18 mg, 75 μmol, 21%) and 2*Z*-(±)-*epi*-AHI1 (50 mg, 0.21 mmol,

59%), respectively, as colorless oils. Data of 2*Z*-*epi*-AHI1. ¹H NMR (500 MHz, CDCl₃): δ 0.76 (3H, d, *J* = 6.7 Hz, H₃-7'), 0.87 (3H, s, H₃-8'), 1.00 (3H, s, H₃-9'), 1.18 (1H, broad d, *J* = 12.8 Hz, H-5' *proS*), 1.35 (1H, m, H-3' *proR*), 1.49 (1H, m, H-3' *proS*), 1.53 (2H, m, H₂-4'), 1.68 (1H, m, H-5' *proR*), 1.91 (1H, ddd, *J* = 12.8, 6.7 and 3.6 Hz, H-2'), 5.65 (1H, d, *J* = 11.3 Hz, H-2), 6.09 (1H, d, *J* = 15.6 Hz, H-5), 6.70 (1H, dd, *J* = 11.3 and 11.3 Hz, H-3), 7.51 (1H, dd, *J* = 15.6 and 11.3 Hz, H-4); ¹³C NMR (125 MHz, CDCl₃): δ 16.4 (C-7'), 21.4 (C-4'), 23.7 (C-9'), 25.5 (C-8'), 29.7 (C-3'), 34.6 (C-2'), 36.0 (C-5'), 38.2 (C-6'), 79.0 (C-1'), 115.8 (C-2), 125.9 (C-4), 146.2 (C-3), 149.9 (C-5), 170.8 (C-1); UV λ_{max} (MeOH) nm (ε): 260.6 (21,900); HRMS (EI) calcd for C₁₄H₂₂O₃ [M]⁺ 238.1569, found 238.1568.

4.7.4. (+)- and (-)-*epi*-AHI1. A Chiralpak AD-H HPLC column (250 × 4.6 mm I.D., Daicel; solvent, 5% 2-propanol in hexane containing 0.1% TFA; flow rate, 1.0 mL min⁻¹; detection, 254 nm) was injected with (±)-*epi*-AHI1 (40 mg, 0.17 mmol). The materials at *t*_R 11.2 and 12.2 min were collected to give (-)-*epi*-AHI1 (19 mg, 80 μmol) and its (+)-enantiomer (19 mg, 80 μmol) with an optical purity of 99.2 and 99.9%, respectively. (-)-*epi*-AHI1: [α]_D²⁸ -57.7 (MeOH; *c* 1.250); (+)-*epi*-AHI1: [α]_D²⁸ +56.6 (MeOH; *c* 1.278).

4.8. Microsomal assay

Kinetic analysis was performed using the detailed protocols described previously.^{8,19,20} Before assay, the inhibitors that were obtained less than 1 mg were re-quantified using the molar absorption coefficient of each compound, which has the same conjugated system. A reaction mixture containing 25 μg mL⁻¹ CYP707A3 microsomes, (+)-ABA (final conc.: 0.5, 1, 2, 4, 8 and 24 μM), inhibitors (0 for control, 0.5-20 μM) and 50 μM NADPH in 50 mM potassium phosphate buffer (pH 7.25) were incubated for 10 min at 30 °C. Reactions were initiated by adding NADPH, and stopped by addition of 50 μL of 1 M HCl. To extract the reaction products, reaction mixtures were loaded onto Oasis HLB

cartridges (1 mL, 30 mg; Waters) and washed with 1 mL of 10% MeOH in H₂O containing 0.5% AcOH. The enzyme products were then eluted with 1 mL of MeOH containing 0.5% AcOH, and the eluate was concentrated in vacuo. The dried sample was dissolved in 50 μ L of MeOH, and 10 μ L were subjected to HPLC. HPLC conditions were: ODS column, YMC Hydrosphere C18 (150 \times 6.0 mm, I.D.); solvent, 40% MeOH in H₂O containing 0.1% AcOH; flow rate, 1.0 mL min⁻¹; detection, 254 nm. Enzyme activity was confirmed by determining the amounts of 8'-hydroxy-ABA (8'-HOABA) and phaseic acid (PA) in control experiments before each set of measurements. The amount of 8'-HOABA was estimated on the basis of a calibration curve for ABA (19, 38, 77, and 191 pmol) because oxygenation at C-8' has little effect on the molar absorbance coefficient of ABA.¹⁶ The amount of PA was determined on the basis of the relative ratio (1.18) of the molar absorption coefficient for 8'-HOABA/PA.³⁴ Inhibition constants were determined using the Enzyme Kinetics module of SigmaPlot 10 software³⁵ after determining the mode of inhibition by plotting the reaction velocities in the presence and absence of inhibitor on a double-reciprocal plot. Values are reported as mean values with standard errors of the entire datasets. For the non-inhibited enzymatic reaction, the K_M for (+)-ABA was calculated to be $0.71 \pm 0.08 \mu\text{M}$, based on 16 separate experiments. All tests were conducted at least three times.

4.9. Isolation of enzyme products of *epi*-AHI1

A reaction mixture containing 25 $\mu\text{g mL}^{-1}$ CYP707A3 microsomes, 10 μM (+)- or (-)-*epi*-AHI1, 50 μM NADPH in 50 mM potassium phosphate buffer (pH 7.25) was incubated for 4 d at 30 $^{\circ}\text{C}$. CYP707A3 microsomes and NADPH were added to the mixture every 2 h and 6 h, respectively. The reaction products were purified described above after being added 50 μL of 1 M HCl to the mixture. The enzyme products were subjected to HPLC under the following conditions: column, YMC Hydrosphere C18 (150 \times 6.0 mm, I.D.); solvent, 45% MeOH (0-10 min), 45-100% MeOH (linear

gradient, 10-37.5 min), 100% MeOH (37.5-43 min) in H₂O containing 0.1% AcOH; flow rate, 1.0 mL min⁻¹; detection, 254 nm. The materials at t_R 20.7 and 22.7 min were collected to give the enzyme products from (-)-*epi*-AHI1 and its (+)-enantiomer, respectively.

4.10. Computational method.

All of the minimum-energy conformers of ABA analogues were generated and minimized using MM3 combined with the molecular dynamics simulation built into CAChe 3.11.³⁶ These MM3-minimized structures were fully optimized with density functional theory, using the Becke three parameter hybrid functional (B3LYP) method and the 6-31G(d) basis set in Gaussian 03,³⁷ followed by a calculation of the harmonic vibrational frequencies at 298 K at the same level. The single point energies were calculated with B3LYP/6-311++G(2df,2p) level of theory. The zero-point energies were scaled by 0.9804.³⁸

Acknowledgment

We thank Toray Industries Inc., Tokyo, Japan, for the gift of (+)-ABA. This research was supported by a Grants-in-Aid for Scientific Research (No. 17-661) from the Ministry of Education, Culture, Sports, Science and Technology of Japan.

References and notes

1. Hirai, N. Abscisic acid. In *Comprehensive Natural Products Chemistry* Vol. 8; Mori, K. Ed.; Elsevier: Amsterdam, 1999; pp 72-91.
2. Davies, W. J.; Jones, H. G. *Abscisic Acid*; BIOS Scientific Publishers: Oxford, 1991.
3. Zeevaart, J. A. D.; Creelman, R. A. *Annu. Rev. Plant Physiol. Plant Mol. Biol.* **1998**, *39*, 439-473.
4. Bruzzone, S.; Moreschi, I.; Usai, C.; Guida, L.; Damonte, G.; Salis, A.; Scarfi, S.; Millo, E.; De Flora, A.; Zocchi, E. *Proc Natl Acad Sci USA.* **2007**, *104*, 5759-5764.
5. Huang, D.; Jaradat, MR.; Wu, W.; Ambrose, S. J.; Ross, A. R.; Abrams, S. R.; Cutler, A. J. *Plant J.* **2007**, *50*, 414-428.
6. Loveys, B. R. In *Abscisic Acid*; Davies, W. J.; Jones, H. G. Eds; BIOS Scientific Publishers: Oxford, 1991.
7. Nambara, E.; Marion-Poll, A. *Annu. Rev. Plant Biol.* **2005**, *56*, 165-185.
8. Saito, S.; Hirai, N.; Matsumoto, C.; Ohigashi, H.; Ohta, D.; Sakata, K.; Mizutani, M. *Plant Physiol.* **2004**, *134*, 1439-1449.
9. Kushiro, T.; Okamoto, M.; Nakabayashi, K.; Yamagishi, K.; Kitamura, S.; Asami, T.; Hirai, N.; Koshiha, T.; Kamiya, Y.; Nambara, E. *ENBO J.* **2004**, *23*, 1647-1656.
10. Yang, S. H.; Choi, D. *Biochem. Biophys. Res. Commun.* **2006**, *350*, 685-690.
11. Yang, S. H.; Zeevaart, J. A. D. *Plant J.* **2006**, *47*, 675-686.
12. Millar, A. A.; Jacobsen, J. V.; Ross, J. J.; Helliwell, C. A.; Poole, A. T.; Scofield, G.; Reid, J. B.; Gubler, F. *Plant J.* **2006**, *45*, 942-954.
13. Destefano-Beltran, L.; Knauber, D.; Huckle, L.; Suttle, J. C. *Plant Mol Biol.* **2006**, *61*, 687-697.

14. Umezawa, T.; Okamoto, M.; Kushiro, T.; Nambara, E.; Oono, Y.; Seki, M.; Kobayashi, M.; Koshihara, T.; Kamiya, Y.; Shinozaki, K. *Plant J.* **2006**, *46*, 171-182.
15. Okamoto, M.; Kuwahara, A.; Seo, M.; Kushiro, T.; Asami, T.; Hirai, N.; Kamiya, Y.; Koshihara, T.; Nambara, E. *Plant Physiol.* **2006**, *141*, 97-107.
16. Todoroki, Y.; Hirai, N.; Koshimizu, K. *Biosci. Biotechnol. Biochem.* **1994**, *58*, 707-715.
17. Todoroki, Y.; Hirai, N.; Koshimizu, K. *Phytochemistry* **1995**, *38* 561-568.
18. Todoroki, Y.; Sawada, M.; Matsumoto, M.; Tsukada, S.; Ueno, K.; Isaka, M.; Owaki, M.; Hirai, N. *Bioorg. Med. Chem.* **2004**, *12*, 363-370.
19. Ueno, K.; Araki, Y.; Hirai, N.; Saito, S.; Mizutani, M.; Sakata, K.; Todoroki, Y. *Bioorg. Med. Chem.* **2005**, *13*, 3359-3370.
20. Ueno, K.; Yoneyama, H.; Saito, S.; Mizutani, M.; Sakata, K.; Hirai, N.; Todoroki, Y. *Bioorg. Med. Chem. Lett.* **2005**, *15*, 5226-5229.
21. Araki, Y.; Miyawaki, A.; Miyashita, T.; Mizutani, M.; Hirai, N.; Todoroki, Y. *Bioorg. Med. Chem. Lett.* **2006**, *16*, 3302-3305.
22. Lin, B. L.; Wang, H. J.; Wang, J. S.; Zaharia, L. I.; Abrams, S. R. *J Exp Bot.* **2005**, *56*, 2935-2948.
23. Razem, F. A.; El-Kereamy, A.; Abrams, S. R.; Hill, R. D. *Nature* **2006**, *439*, 290-294.
24. Shen, Y. Y.; Wang, X. F.; Wu, F. Q.; Du, S. Y.; Cao, Z.; Shang, Y.; Wang, X. L.; Peng, C. C.; Yu, X. C.; Zhu, S. Y.; Fan, R. C.; Xu, Y. H.; Zhang, D. P. *Nature* **2006**, *443*, 823-826.
25. Liu, X.; Yue, Y.; Li, B.; Nie, Y.; Li, W.; Wu, W. H.; Ma, L. *Science* **2007**, *315*, 1712-1716.

26. Ortiz de Montellano, P. R. ed.; *Cytochrome P450: Structure, mechanism, and Biochemistry*, 3rd ed.; Kluwer Academic/Plenum Publishers, New York, 2005.
27. Lamb, N.; Abrams, S. R. *Can. J. Chem.* **1990**, *68*, 1151-1162.
28. Oritani, T.; Yamashita, K. *Agric. Biol. Chem.* **1974**, *38*, 801-808.
29. Oritani, T.; Yamashita, K. *Agric. Biol. Chem.* **1970**, *34*, 830-837.
30. Sundaresan, V.; Abrol, R. *Chirality* **2005**, *17*, S30-S39.
31. Zaharia, L. I.; Gai, Y.; Nelson, K. M.; Ambrose, S. J.; Abrams, S. R. *Phytochemistry* **2004**, *65*, 3199-3209.
32. Kondo, S.; Ponrod, W.; Kanlayanarat, S.; Hirai, N. *Plant Growth Regul.* **2003**, *39*, 119-124.
33. Hirai, N.; Okamoto, M.; Fujimura, M.; Ichiyama, T.; Todoroki, Y.; Ohigashi, H.; Takeda, N.; Yoshizumi, H.; Tatematsu, A. *J. Mass Spectrom. Soc. Jpn.* **2000**, *48*, 8-22.
34. Todoroki, Y.; Hirai, N.; Ohigashi, H. *Tetrahedron* **2000**, *56*, 1649-1653.
35. *SigmaPlot 10*; Systat Software, Inc.: Richmond CA, 2006.
36. *CAChe, 3.11*; Oxford Molecular Ltd.: London, 1998.
37. *Gaussian 03 Revision D.01*; Gaussian, Inc.: Wallingford CT, 2004.
38. Bauschlicher, Jr., C. W.; Partridge, H. *J. Chem. Phys.* **1995**, *103*, 1788-1791.

Table 1. Inhibition constants for both enantiomers of AHI1, 6-nor-ABA, enone modified ABA analogues and *epi*-AHI1 of recombinant CYP707A3

| Compounds | K_i [μ M] | |
|----------------------------|-------------------|-----------------|
| | (+)-enantiomer | (-)-enantiomer |
| AHI1 | 1.28 ± 0.32 | 0.30 ± 0.04 |
| 6-Nor-ABA | 0.16 ± 0.01^a | NI ^b |
| 2',3'-Dihydro-ABA | 5.80 ± 1.33 | NI |
| 4'-Deoxo-ABA | 2.32 ± 0.49 | 27.2 ± 8.8 |
| 2',3'-Dihydro-4'-deoxo-ABA | 5.27 ± 0.84 | 0.45 ± 0.11 |
| <i>epi</i> -AHI1 | 2.50 ± 0.54 | 1.63 ± 0.82 |

^a Published value.¹⁹

^b No measurable inhibition.

Table 2. Conformational energy profiles of 2',3'-dihydro-ABA, 4'-deoxo-ABA, 2',3'-dihydro-4'-deoxo-ABA, and *epi*-AHI1

| Compounds | relative total energy ^a [kcal mol ⁻¹] |
|----------------------------|---|
| 2',3'-Dihydro-ABA | - 2.91 |
| 4'-Deoxo-ABA | - 1.02 |
| 2',3'-Dihydro-4'-deoxo-ABA | - 3.71 |
| <i>epi</i> -AHI1 | +4.78 |

^a Values are the relative total energies of a chair form with the axial side chain when energies of a chair form with the equatorial side chain are set to zero. Total energies are based on single point energies plus zero-point energies. Geometry optimizations and frequencies were calculated at the B3LYP/6-31G(d) level of theory, and single point energies were calculated at the B3LYP/6-311++G(2df,2p) level of theory.

Figure and Table Legends

Figure 1. Structural properties of optically pure ABA and AHI1. (A) 2D-structures of both enantiomers. The arrow indicates the site of oxidation by CYP707A3. (B) 3D-structures of both enantiomers and their overlay structures. In the stick models, carbons, hydrogens, and oxygens are colored grey, white, and red, respectively. In the overlay structures, the (+)-enantiomer is depicted in blue, whereas the (–)-enantiomer is depicted in red.

Figure 2. Determination of the absolute configuration of (+)-AHI1 (red and green arrows) and synthesis of enone-modified ABA analogues: (1'*S*',2'*S*')-2',3'-dihydro-ABA, 4'-deoxo-ABA and (1'*S*',2'*S*')-2',3'-dihydro-4'-deoxo-ABA (blue and green arrows). The absolute configuration of (+)-AHI1 was determined by the chemical correlation method. To clarify the configuration at C2', the synthetic scheme of enone-modified ABA analogues was depicted using (1'*S*')-enantiomer. Compound **3** was a diastereomeric mixture derived from the stereochemical impurity at C4'. The optically pure enone-modified compounds were gained by optical resolution of the racemates or synthesis from (+)-ABA. Reagents: (i) NaIO₄, OsO₄; (ii) MeMgBr; (iii) PDC, Celite; (iv) NaBH₄; (v) ClC(S)OPh, 4-DMAP; (vi) *n*-Bu₃SnH, AIBN; (vii) NaOH; (viii) ClCO₂Me, 4-DMAP; and (ix) [Pd₂dba₃]·CHCl₃, *n*-Bu₃P, NaBH₄. DMAP, dimethylaminopyridine; AIBN, 2,2'-azobisisobutyronitrile; dba, dibenzylideneacetone.

Figure 3. Favored conformations of 2',3'-dihydro-ABA, 4'-deoxo-ABA, and 2',3'-dihydro-4'-deoxo-ABA. Blue arrows represent the observed NOEs.

Figure 4. Competitive inhibition of CYP707A3 by (–)-2',3'-dihydro-4'-deoxo-ABA (A), (–)-4'-deoxo-ABA (B) and (+)-*epi*-AHI1 (C). Assays contained (+)-ABA (open square), (+)-ABA and indicative concentration of ABA analogues (0.5 μM, 20 μM and 4 μM in A, B and C, respectively; closed triangle). The inset is a double reciprocal plot of the same data.

Figure 5. Structure and synthesis of racemic *epi*-AHI1. (A) 2D- and 3D-structure of (1'*S*,2'*R*)-*epi*-AHI1. In the stick model, carbons, hydrogens, and oxygens are colored grey, white, and red, respectively. (B) The route of *epi*-AHI1 synthesis. Although all compounds are racemates, one enantiomer is shown to indicate the relative configurations. Acetylide anion attack to trimethylcyclohexanone generated two diastereomers at a ratio of 10:1; the major diastereomer whose relative configuration is (1'*S**,2'*S**) was converted to AHI1 described previously (ref. 20), whereas the minor, (1'*S**2'*R**)-diastereomer **6** was converted to *epi*-AHI1 via compound **7**. Reagents: (i) *n*-BuLi, 2-propynyl-TBS ether; (ii) SMEAH; (iii) AcOH:H₂O (3:1, v/v); (iv) PDC, Celite; (v) ethyl di-*o*-tolylphosphonoacetate, NaH; (vi) NaOH.

Table 1. Inhibition constants for both enantiomers of AHI1, 6-nor-ABA, enone modified ABA analogues and *epi*-AHI1 of recombinant CYP707A3

Table 2. Conformational energy profiles of 2',3'-dihydro-ABA, 4'-deoxo-ABA, 2',3'-dihydro-4'-deoxo-ABA, and *epi*-AHI1

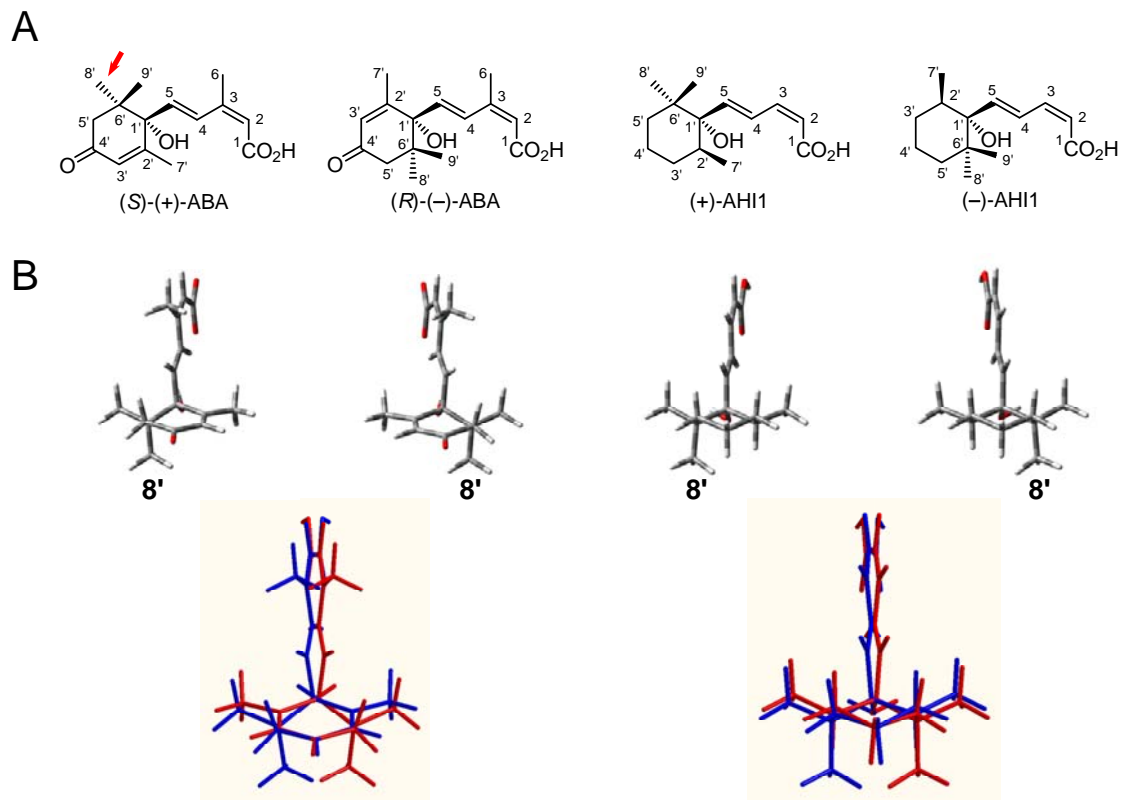


Figure 1

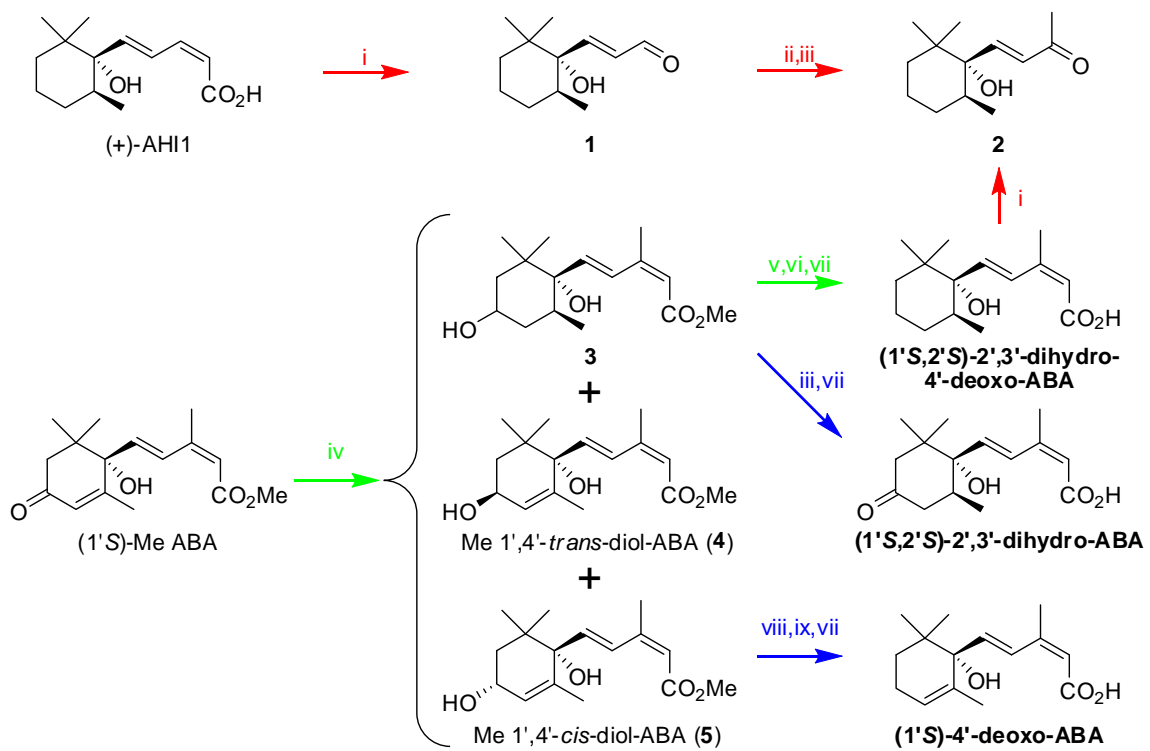
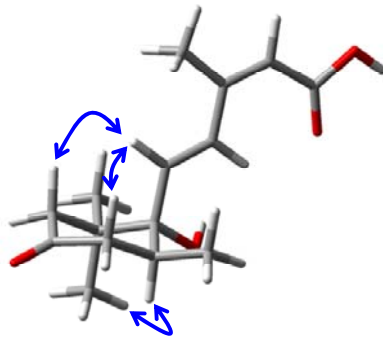
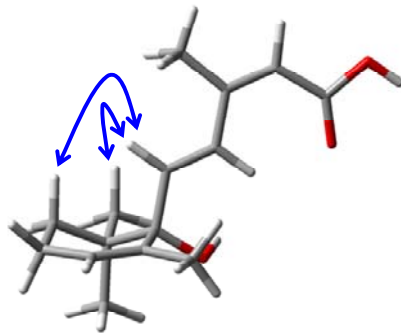


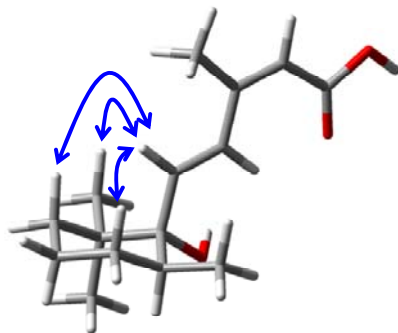
Figure 2



2',3'-dihydro-ABA



4'-deoxy-ABA



2',3'-dihydro-4'-deoxy-ABA

Figure 3

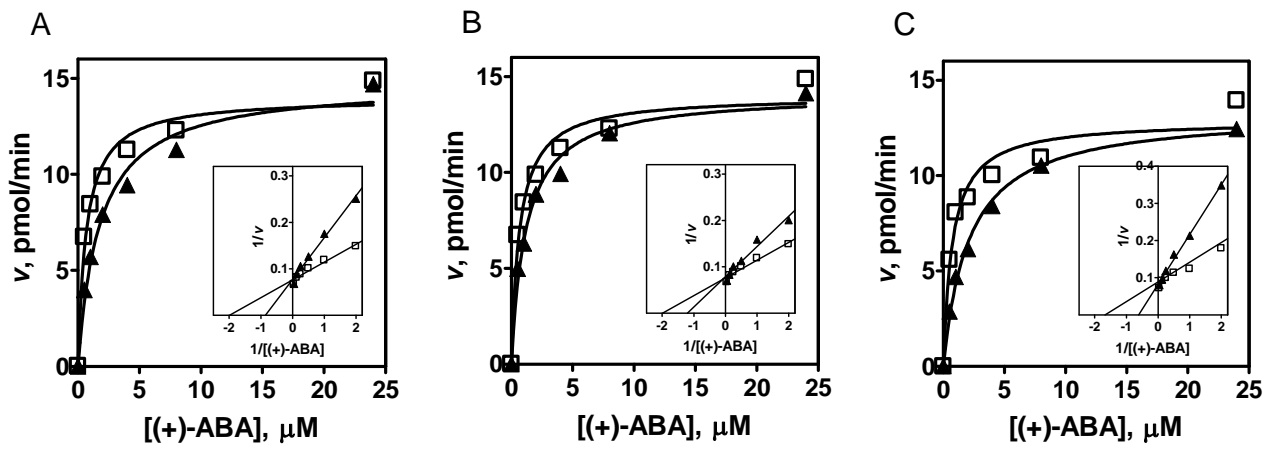


Figure 4

A



B

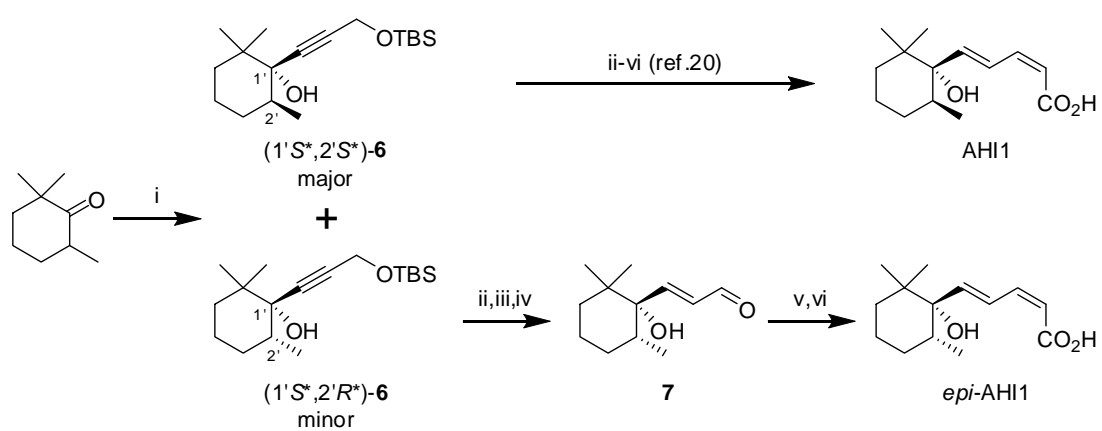


Figure 5